Liquid Crystals

Publication details, including instructions for authors and subscription information:
http://www.informaworld.com/smpp/title~content=t713926090

AFM study of forces in and structures of nematic liquid crystal interfaces on silanated glass

K. Koevar; I. Muevi

To cite this Article Koevar, K. and Muevi, I.(2001) 'AFM study of forces in and structures of nematic liquid crystal interfaces on silanated glass', Liquid Crystals, 28: 4, 599 — 606

To link to this Article: DOI: 10.1080/02678290010020184

URL: http://dx.doi.org/10.1080/02678290010020184

LIQUID CRYSTALS, 2001, VOL. 28, NO. 4, 599–606

AFM study of forces in and structures of nematic liquid crystal interfaces on silanated glass

K. KOČEVAR† and I. MUŠEVIČ*†‡

†J. Stefan Institute, Jamova 39, 1000 Ljubljana, Slovenia
‡Faculty of Mathematics and Physics, University of Ljubljana, Jadranska 19,
1000 Ljubljana, Slovenia

(*Received 9 June 2000; accepted 14 October 2000*)

We have studied interfacial forces in MBBA, 5CB, 8CB and 12CB liquid crystals on DMOAP silanated glass substrates using a temperature controlled AFM in the force spectroscopy mode. In the bulk isotropic phase all these interfaces are clearly divided into two regions. The first molecular layer, which is absorbed to the glass surface, is smectic-like and shows submicron holes; this layer covers approximately 70% of the surface and is in all cases stable far beyond the clearing point. It is followed by a partially ordered region, which is different for different materials. We observe pre-nematic ordering in 5CB, pre-smectic ordering in 8CB and well developed layer-by-layer ordering in 12CB.

1. Introduction

The structure of liquid crystal interfaces on solid substrates has been a subject of great technological and fundamental interest in recent years [1]. From the technological point of view, these interfaces are important parts of liquid crystal devices and an understanding of the physical mechanisms that align liquid crystals on solids or polymers is crucial for liquid crystal technology. On the other hand, the behaviour of liquid crystals in confined geometries, and wetting phenomena at surfaces, have also attracted much attention due to their fascinating richness. This has stimulated numerous X-ray [2], NMR [3], non-linear optical [4], ellipsometric [5], STM [6], SFA [7] and other studies (for a review see [1]).

In many cases it was observed that the aligning action of the substrate is mediated by the first molecular layer that is in close proximity to the substrate [4, 8]. This is directly manifested in the so-called memory effect, where a particular liquid crystalline texture is observed even after heating the interface far above the isotropic phase transition point [8]. The memory effect was explained on the basis of the so-called first molecular layer: this is a layer of liquid crystal molecules that is strongly adsorbed to the solid surface and remains stable on heating the bulk material into higher temperature phases or even the isotropic phase. This layer was first directly detected in the non-linear optical studies of 8CB on polymer-coated glass substrates (see Ouchi *et al.* [8]). The experiment showed the presence of a polar molecular layer of 8CB, which was very stable to increasing temperature. Indirectly, the presence of a first molecular layer was detected in ellipsometric [5] and NMR experiments [3] on cyanobiphenyls on solid substrate. In these cases, the extra, surface-adsorbed layer was necessary to explain the shape and temperature dependence of the NMR or ellipsometric spectra.

Up to now, there has been no '*in situ*' AFM study of 'buried' interfaces between a nematic liquid crystal and a solid substrate. The experimental problem here is that the interface is buried under bulk liquid crystal above the interface and it is therefore difficult to image and access. We have solved this problem by using a temperature controlled AFM [9], where bulk liquid crystal above the interface is kept in the isotropic phase, whereas the temperature of the interface is allowed slowly to approach the clearing point from above. The AFM was used in the so-called force spectrometry mode, and we have studied the temperature dependences of the interfacial forces in the nematic liquid crystals 5CB, 8CB, 12CB and MBBA on DMOAP silanated glass. In this mode of operation, the forces on the AFM tip were measured as a function of the separation between a solid surface and the AFM tip. The force profiles obtained reflect the structure of the interface [10] and were interpreted using Landau-de Gennes formalism [11, 12].

We have observed the following.

(i) In all materials we have detected the first molecular layer. The thickness of this layer is close to the length of the fully extended liquid

---

*Author for correspondence; e-mail: igor.musevic@ijs.si

Liquid Crystals ISSN 0267-8292 print/ISSN 1366-5855 online © 2001 Taylor & Francis Ltd
http://www.tandf.co.uk/journals
DOI: 10.1080/02678290010020184

crystal molecule used in the particular experiment. It is stable more than 20 K above the clearing point, which indicates strong adsorption of the liquid crystal molecules to the glass surface.

(ii) The first molecular layer can be elastically deformed on pressing it with a sharp tip, and it ruptures at a maximum load of 50 pN across a 20 nm tip. The corresponding elastic modulus of the first layer is of the order of $E = 10^7$ N m^{-2}, which is close to the elastic compressibility modulus B of smectics.

(iii) The first molecular layer is laterally inhomogeneous; holes of submicron scale are randomly distributed across the interface.

(iv) The first molecular layer is followed by a prenematic layer in 5CB, a smoothly decaying presmectic modulation in 8CB and a layer-by-layer sequence in 12CB.

2. Experimental

In our experiments we have used a temperature controlled atomic force microscope [9], shown schematically in figure 1 (*a*). The AFM has a double temperature control and can be used to measure and image liquid crystal interfaces above the clearing point. The temperature of the liquid crystal is controlled within 5 mK by a small heater, attached directly to the piezo scanner of the AFM. The second micro-heater is attached above the AFM cantilever to reduce the temperature gradients in the liquid crystal which fills the space between the lower glass plate and the upper heater. In this geometry, the AFM cantilever and the AFM probe are completely immersed in liquid crystal and there are no capillary forces. We have used two different AFM probes to expand the accessible range of forces exerted on the surface. In the first set of experiments, cantilevers with a sharp Si_3N_4 tip (Park Scientific) were used. The force constants of the cantilevers ranged from 0.01 to 0.1 N m^{-1} and the radius of the tip was typically 20 nm. Using these sharp cantilevers, relatively large force loads can be applied to the interfacial structure and one can eventually detect (and image) the surface-adsorbed layers of molecules. In other experiments, a micrometer-sized glass sphere was attached to the cantilever, figure 1 (*b*), and the force beween the sphere and the flat surface was measured with nematic liquid crystal in between.

The glass substrates and glass spheres were carefully cleaned in detergent, rinsed in pure water and cleaned in acid. After rinsing with pure water, a monolayer of DMOAP (*N*,*N*-dimethyl-*N*-octadecyl-3-aminopropyltrimethoxysilyl chloride), was deposited on the glass surfaces from a water–alcohol solution, as described elsewhere. This gave an excellent and stable homeotropic alignment of nematic liquid crystal, as checked by polarizing optical microscopy on separate samples. The AFM sharp probes were used with no modifications and cleaning. New AFM probes were used for each experiment.

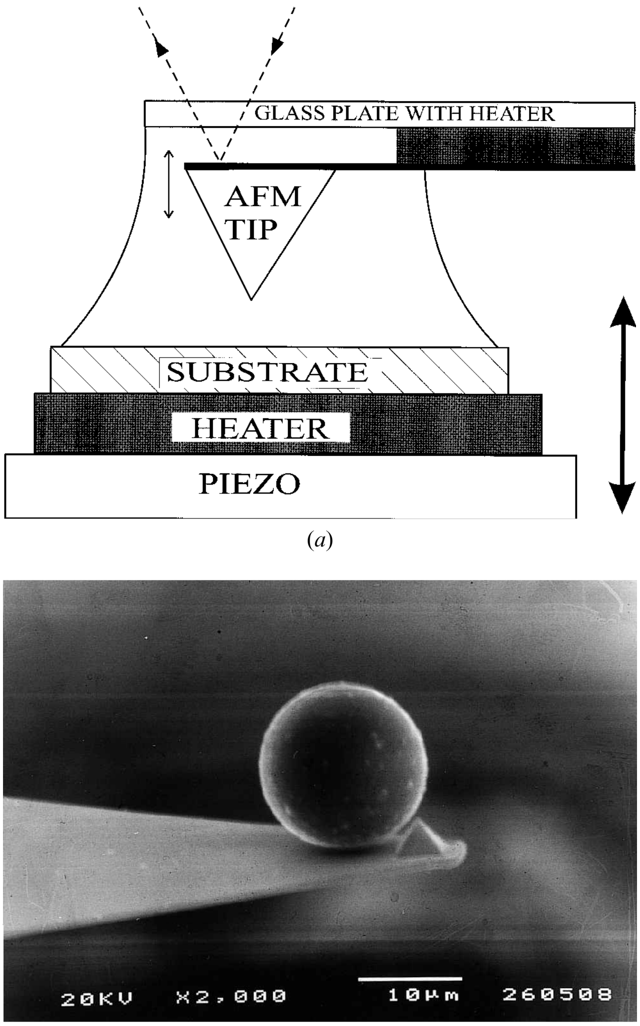

(*a*)

(*b*)

Figure 1. (*a*) Details of the temperature controlled AFM set-up. (*b*) Electron microscope image of a micron sphere attached to the AFM cantilever.

The AFM was used in the so-called force plot mode of operation, where the piezo scanner of the AFM and the substrate perform time-periodic linear movements in the direction of the AFM tip. The speed of approach is several nm per second; at the same time the deflection of the AFM cantilever is monitored, giving force versus separation plots. Zero separation was determined from the point of hard contact between the sharp AFM probe and the substrate.

3. Results and discussion

3.1. *Forces mediated by the DMOAP monolayer and the first molecular layer*

A typical force plot using a sharp AFM tip is shown in figure 2; this was measured at a DMOAP–MBBA interface, in the isotropic phase. At large separations, the force on the AFM tip is zero. When the tip approaches to a distance of several molecular lengths (point A in figure 2), it is suddenly strongly attracted towards the surface and comes into equilibrium at a separation somewhat larger than the length of a single molecule (point B in figure 2). After that, the tip starts compressing the material (B–C) and the forces necessary to compress the material increase strongly with decreasing separation (C–D). Finally, at some critical distance (point D in figure 2), the tip ruptures the material and comes into hard contact with the substrate (E). We can clearly see that the thickness of fully compressed layer is of the order of a molecular length and can be attributed to the first adsorbed layer of liquid crystal molecules, which are homeotropically anchored to the surface. The deformation of this layer is purely elastic. Using the Hertz continuum theory of indentation of a soft layer of material with a sphere of radius R [13], we calculate the elastic modulus of this first layer to be of the order of $E \approx 10^7$ N m^{-1}. This is close to the compressibility modulus of smectics and gives a hint that the first molecular layer is smectic-like.

We have excluded the other possibility that the observed first layer is a DMOAP layer by the following experiment. We used hexane instead of liquid crystal and figure 3 shows the corresponding force plot for

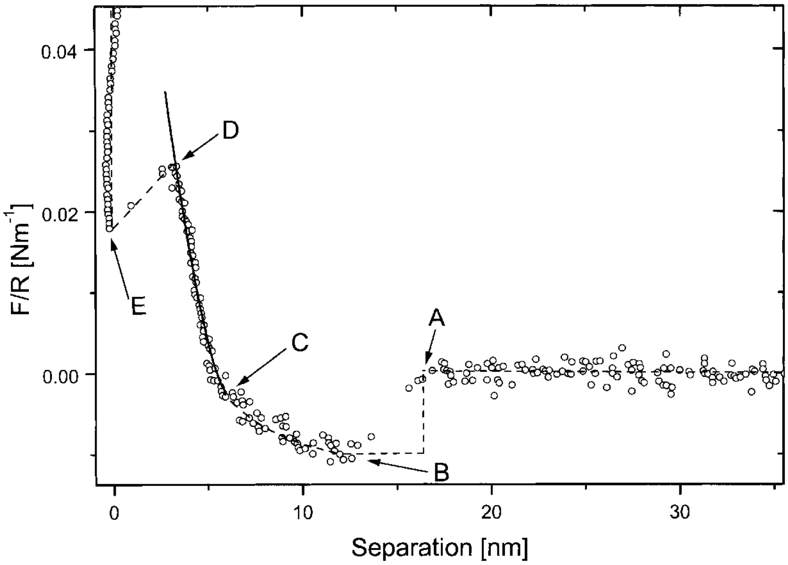

Figure 2. The force on the Si_3N_4 AFM tip, normalized to the tip radius $R = 20$ nm, as a function of separation between the tip and the DMOAP silanated glass surface in the bulk isotropic phase of MBBA, several degrees above T_c. The solid line is the fit to Hertz theory with compressibility modulus $E = 1.6 \times 10^7 (1 \pm 0.15)$ N m^{-2}.

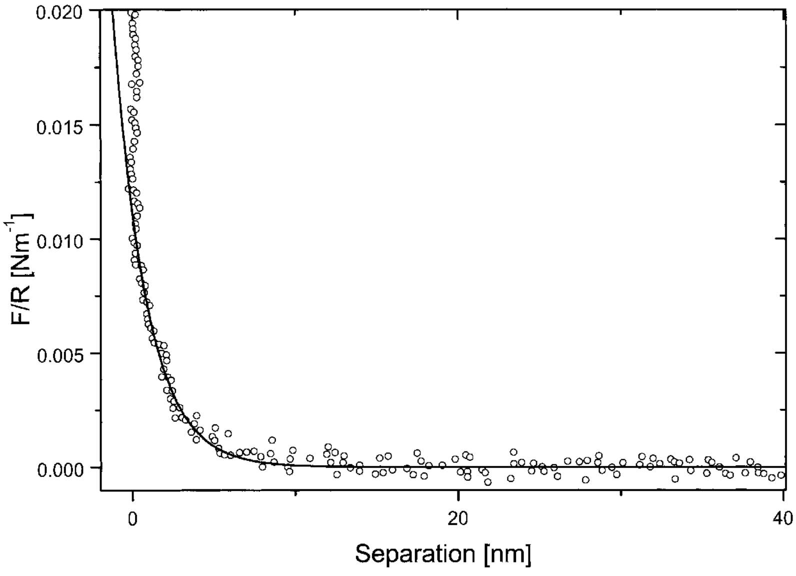

Figure 3. The force on the Si_3N_4 AFM tip, normalized to the tip radius $R = 20$ nm, as a function of separation between the tip and the DMOAP silanated glass surface in the presence of hexane at room temperature. The solid line is the exponential fit with decay length 2 nm. The length of the fully extended DMOAP molecule is 2.9 nm.

the hexane–DMOAP interface. The interfacial forces are short ranged and are of the same order of magnitude as those observed for the liquid crystal–DMOAP interface. There are however two important differences. First, the separation dependence of the force is quite different and can be well described by an exponentially decaying force with a decay distance of 2 nm. Second, the layer is never ruptured by the tip, but merely compresses to a very thin layer. This clearly indicates that the DMOAP molecules are strongly positionally anchored and cannot move away from the AFM tip under an applied force. We therefore conclude that in the previously mentioned experiments we indeed observe compression and rupture of the first adsorbed layer of liquid crystal molecules. This layer is observed in 5CB, 8CB, 12CB and MBBA.

When measuring force plots at different places on the substrate, we have observed that the characteristic 'step' in the force plot is observed in some places, whereas it cannot be observed in others. This has led to the conjecture that the first molecular layer is not laterally homogeneous, but appears in the form of smectic clusters. By performing a large number of force plots (i.e, volume force lots) across the interface, we observe a characteristic pattern, shown in figure 4 for 8CB. Here, the field of view is 5 by 10 μm and force plots have been performed at equidistant points. Dark points indicate the absence of the first molecular layer (i.e. voids), whereas light points indicate the presence of the first molecular layer. Lateral inhomogeneities are clearly evident and are observed across a typical distance of 0.1–0.5 μm.

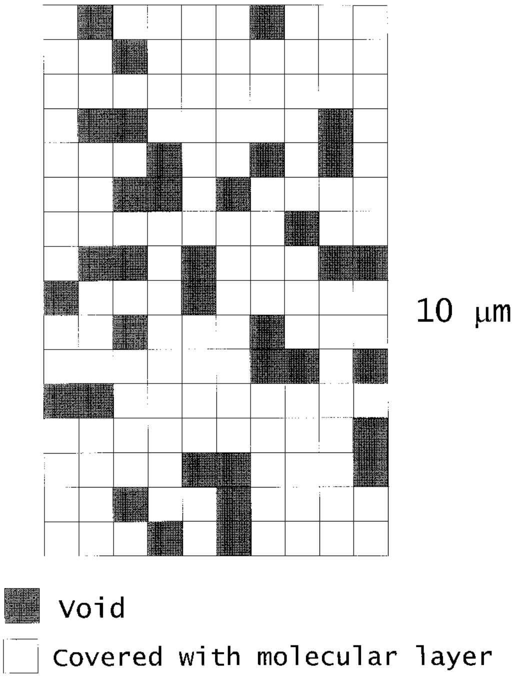

Figure 4. Volume force plot of the 8CB–DMOAP interface. Light regions represent the presence of an elastic first molecular layer, which is detected by performing a force plot at that place. In the dark regions, there is no first molecular layer. The field of view is 5 by 10 μm^2.

We have imaged the first molecular layer in the contact AFM mode, with the result shown in figure 5 for MBBA on DMOAP. Most of the surface is covered with a 2–3 nm thick layer of liquid crystal molecules, whereas one can clearly see 'voids' of 100–500 nm lateral size where this first smectic-like layer is absent. We have therefore a general situation, where the DMOAP aligning layer is incompletely wetted by a smectic-like first molecular layer, which forms a 'cheese-like' surface cover. This layer is followed either by a pre-nematic or pre-smectic region, depending on the characteristics of the bulk liquid crystal. In materials where the nematic phase is very narrow (8CB) we observe pre-smectic ordering following the first molecular layer, whereas in materials with no smectic phase (5CB) we observe pre-nematic order, as will be shown later in the paper.

3.2. *Pre-nematic forces at the 5CB–DMOAP interface*

Forces mediated by pre-nematic or pre-smectic surface-induced order are too small to be detected with a sharp AFM tip. We therefore use a tip with an attached glass microsphere, as shown in figure 1 (*b*), and measure the separation dependence of the force on a microsphere, as it approaches the DMOAP interface. The results are shown in figure 6 for 5CB on a DMOAP glass surface at two different temperatures above the clearing point. One can clearly see an attractive force between the two surfaces, decaying approximately exponentially with increasing separation. The decay length is approximately 5–10 nm, which is close to the correlation length in 5CB at these temperatures. At higher temperatures, the magnitude and range of this force are somewhat smaller. This is a clear indication that this attractive force is mediated by surface-induced pre-nematic ordering, as discussed theoretically by various authors [14]. For small values of the surface-induced nematic order, the mean-field attractive force on a sphere with radius R is [12]

$$F(D)_{\mathrm{sphere}} = 2\pi R\alpha(T)\xi(T)S_{\mathrm{o}}^2\left\{\mathrm{th}\left[\frac{D}{2\xi(T)}\right]-1\right\}. \qquad (1)$$

Here we have used the Derjaguin approximation [10], which is valid as long as the range of the force ξ and the separation D between the two surfaces are small compared to the radius R. The temperature dependent coefficient $\alpha(T) = a(T - T^*)$ drives the weakly first order *isotropic–nematic* transition, whereas S_{o} is the value of

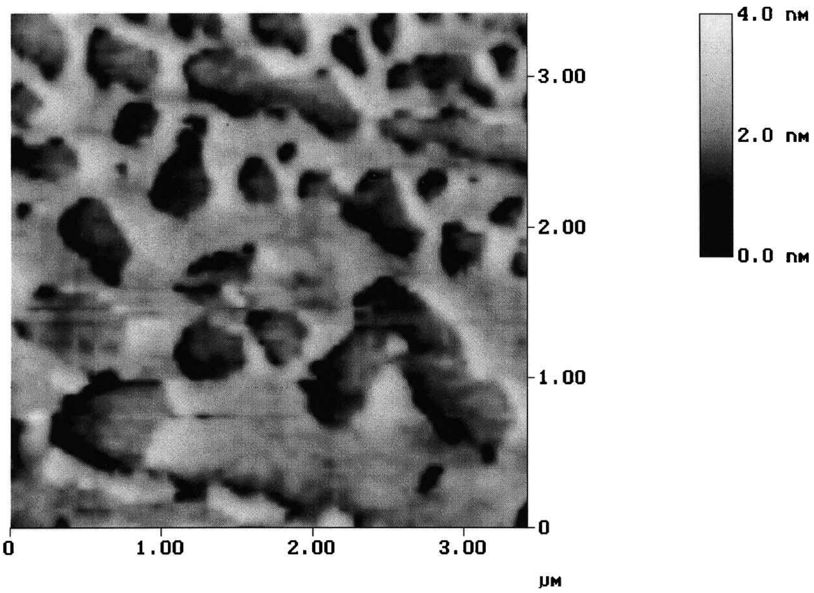

Figure 5. Image of the first molecular layer of MBBA at the DMOAP interface. The image was taken in the contact mode several degrees above the isotropic–nematic phase transition of the bulk material. Note that this image was taken by an AFM tip immersed in the bulk liquid crystal, which is above this first molecular layer.

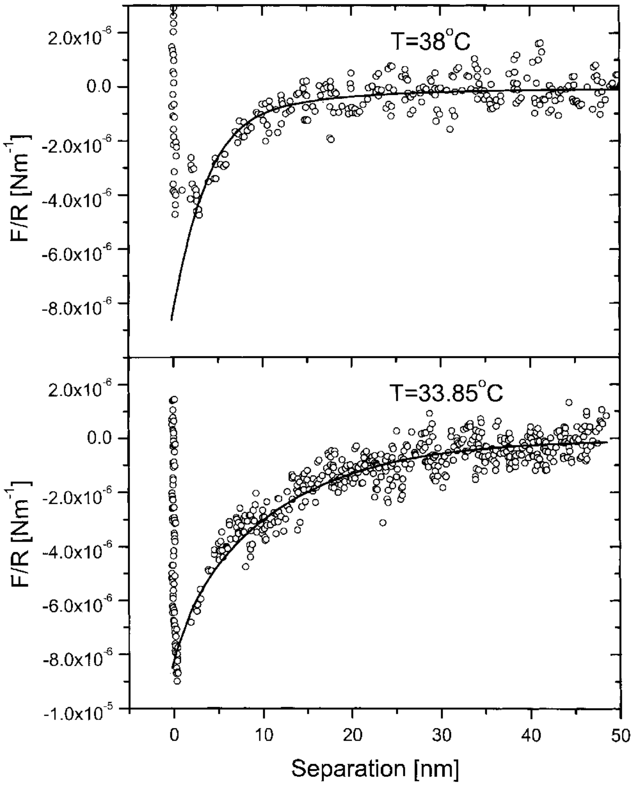

Figure 6. Force plot for a 5CB–DMOAP interface. The attractive force on a micrometer-sized sphere attached to the AFM cantilever is due to a combination of van der Waals and nematic mean-field forces (Eq. 1), shown by the solid line; see equation (1). Note that this attractive force is temperature dependent.

the nematic order parameter at the surface. The force, which is mediated by the surface-induced nematic order parameter, is attractive and decays approximately exponentially with increasing separation D. The solid line in figure 6 is the fit to equation 1, using Landau parameters for 5CB (see Ziherl *et al.* [3]). We have added a small van der Waals attraction, with Hamaker constant 1×10^{-21} J calculated from the dielectric and optical data for glass and 5CB. The results of the fit yield a bare nematic correlation length $\xi_o = 0.66$ nm and the value of the nematic order parameter at the surface $S_o = 1.5 \times 10^{-2}$. The nematic correlation length is in good agreement with that from ellipsometric data (see Hsiung *et al.*, [5]), whereas S_o is nearly an order of magnitude smaller. We have made independent ellipsometric experiments on the same system, which give similar value of S_o, as deduced from the force experiments. The conclusion is that we have indeed observed an attractive mean-field force due to surface-induced pre-nematic order.

3.3. *Pre-smectic forces at the 8CB–DMOAP interface*

The results of the force spectroscopy on the 8CB–DMOAP interface are quite different, as shown in figure 7. Instead of the smooth force profile observed for 5CB, we observe an oscillatory force profile, indicating pre-smectic ordering of 8CB on the DMOAP surface. The amplitude of oscillation is larger as we approach the nematic phase transition from above, and the range of the oscillations increases. The range of the oscillations is several molecular lengths, and is of the order of a smectic correlation length of 8CB on the DMOAP surface. The force profile was fitted with an expression first derived by de Gennes [11], and later used by Moreau *et al.* [15], who observed similar force profiles in the isotropic phases of lyotropic crystals. In the Derjaguin

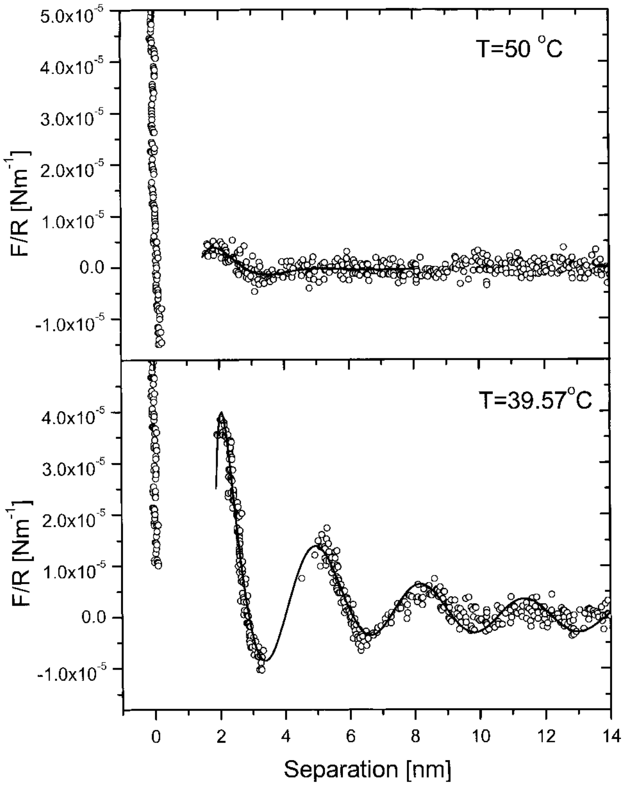

Figure 7. The normalized structural force as a function of separation between a 6.2 μm silanated glass sphere and a flat silanated glass surface in the bulk isotropic phase of 8CB, at different temperatures. The solid line in the lower graph is the best fit to the equation (2) with $\psi_s = 0.04\ (1 \pm 0.05)$, $d_a = 3.2\ (1 \pm 0.015)$ nm and $\xi_\parallel = 2.9\ (1 \pm 0.15)$ nm.

approximation, this structure force is [15]:

$$F = 2\pi R \alpha \xi_\parallel \rho_s \left\{ \tanh[(d - d_a)/2\xi_\parallel] + \frac{1 - \cos[\Phi]}{\sinh[(d - d_a)/\xi_\parallel]} - 1 \right\}. \qquad (2)$$

Here, d_a is the zero-stress separation without any intermediate smectic layer. $\Psi = \psi \exp(i\Phi)$ is the smectic order parameter, ψ measuring the amplitude of modulation, and $\Phi = (2\pi/a_o)u$ is the phase related to layer displacement u and smectic periodicity a. $[\Phi] = \Phi(d/2) - \Phi(-d/2) = 2\pi(d = na_o)/a_o$ is the phase difference that gives rise to strain when the distance d between the surfaces is not an integral multiple of a_o. $\rho_s = \psi_s^2$ is the smectic density at the surface. $\xi_\parallel$ is the smectic correlation length and $\alpha = a(T - T_o)$ is the coefficient of the harmonic term of the Landau expansion, driving the *nematic–smectic A* transition.

The modelling force is in good quantitative agreement with experiment and allows for a determination of the smectic order ψ_s at the surfaces, the smectic correlation length $\xi_\parallel$, and the smectic periodicity a. We obtain from the data in figure 7 the smectic amplitude at the surface $\psi_s = 0.04(1 \pm 0.05)$, the smectic correlation length $\xi_\parallel = 2.9(1 \pm 0.15)$ nm, the zero stress separation $d_a = -0.8(1 \pm 0.2)$ nm and a smectic periodicity $a_o = 3.2(1 \pm 0.015)$ nm. This is in excellent agreement with bulk values [16] and indicates bilayer pre-smectic ordering.

3.4. *Smectic forces at the 12CB–DMOAP interface*

The force profiles obtained at the 12CB–DMOAP interface in the bulk isotropic phase are shown in figure 8 and are quite different from those for 5CB and 8CB. The force profiles, taken at different temperatures, clearly show well defined steps that correspond to rupturing of smectic layers and directly reflect the tendency of 12CB to form the smectic phase. The width of a single step is 3.9 nm and equals the thickness of a single smectic bilayer of 12CB [16]. The number of smectic layers increases as the temperature is lowered towards the clearing point from above. This is consistent with X-ray experiments of Ocko [2], who observed layer-by-layer growth of 12CB on an alkylsilane-coated silicon. The rupturing force increases with decreasing temperature,

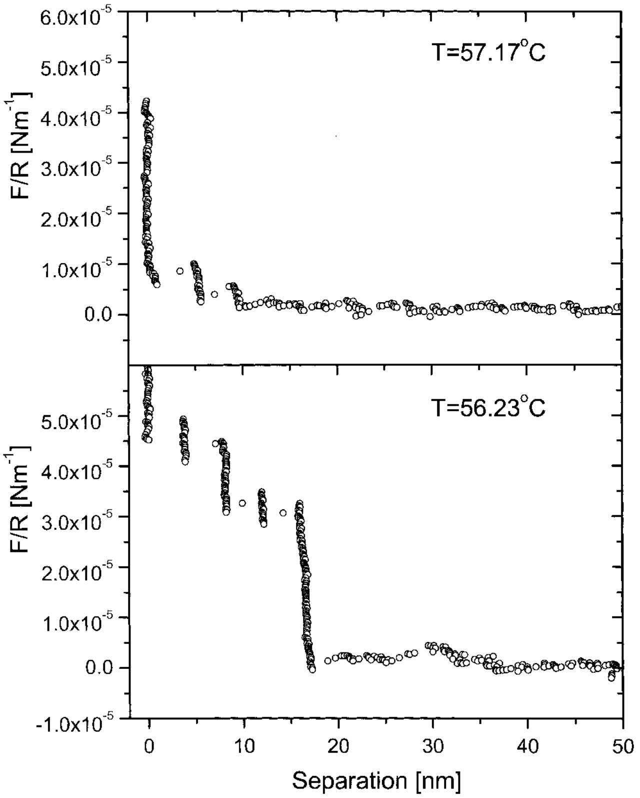

Figure 8. The normalized structural force as a function of separation at the 12CB–DMOAP interface, taken at different temperatures above the isotropic phase transition. Note an increased number of smectic layers when the temperature approaches the clearing point.

which means that the smectic order parameter of the pre-smectic layers grows as we approach the smectic phase from the isotropic phase.

4. Conclusions

In conclusion, we have shown that AFM in the force spectroscopy mode can be used very efficiently to extract important quantitative data on the structure of nematic interfaces on solids. Our experiments on the structure of glass–DMOAP–cyanobiphenyl interfaces lead to the following conclusions:

(i) In 5CB, 8CB, MBBA and 12CB there is always a first layer of molecules, strongly adsorbed to the DMOAP–glass surface. The thickness of this layer is close to the length of a single liquid crystal molecule. It is smectic-like, and is stable far above the clearing point. This layer is responsible for the 'memory effect' in liquid crystals.

(ii) The first molecular layer is laterally inhomogeneous, as it clearly shows submicron-sized voids and covers approximately 70% of the interface. There are two possible explanations for this incomplete coverage. The first is the relatively low surface energy of the liquid crystal on DMOAP, which can be a reason for incomplete wetting of DMOAP by smectic order. The second possibility is inhomogeneities in the glass surface which are of a size similar to the size of the voids.

(iii) In 5CB, the first smectic-like molecular layer is followed by a weak pre-nematic order, with a nearly undetectable smectic modulation. The nematic surface order parameter is $S_o = 0.015$ and is temperature independent. In some experiments, we observe very weak smectic modulation, which is however smaller than $\psi < 10^{-5}$.

(iv) In 8CB, the first smectic-like molecular layer is followed by a pre-smectic modulation, which is strongly temperature dependent. Smectic order of the first layer is estimated as $\psi_1 \approx 0.3$, whereas the amplitude of the smectic order in the pre-smectic region is $\psi_s \approx 0.04(1 \pm 0.05)$ and this decays with a smectic correlation length as we move into the isotropic bulk. AFM can therefore be used to detect the smectic order parameter and surface correlation lengths.

(v) In 12CB, the first molecular layer is followed by a discrete sequence of well developed smectic bilayers. The number of smectic layers decreases with increasing temperature.

These observations have several implications for the interpretation of wetting experiments and theory. The experiments show that many wetting phenomena in liquid crystals may be in reality much more complicated than was previously assumed. The first complication arises from the presence of the first molecular layer, which is adsorbed to the surface. The question is to what extent this first molecular layer dictates the wetting mechanism. Does the interior of a liquid crystal 'see' the surfactant at the surface or does it merely see the first adsorbed layer? Secondly, liquid crystal interfaces on glass and other amorphous substrates seem to be highly laterally inhomogeneous, which can have a strong influence on the interpretation of wetting experiments. Thirdly, there is obviously an intrinsic, strong coupling between the smectic and nematic order parameters in materials that have a very narrow nematic phase, followed by a smectic phase. This coupling induces pre-smectic modulation near a flat surface already in the isotropic phase of a nematic liquid crystal material. The question whether these observations are related only to particular properties of glass and other amorphous surfaces, or are observable on atomically smooth surfaces as well, has to be answered by future AFM experiments on atomically well-defined surfaces.

References

[1] Jerome, B., 1991, *Rep. Prog. Phys.*, **54,** 391; Collings, P. J., Patel, J. S. (editors), 1997, *Handbook of Liquid Crystal Research* (Oxford University Press).

[2] Ocko, B. M., 1990, *Phys. Rev. Lett.*, **64,** 2160; Ocko, B. M., Braslau, A., Pershan, P. S., Als-Nielsen, J., and Deutsch, M., 1986, *Phys. Rev. Lett.*, **57,** 94; Iannacchione, G. S., Mang, J. T., Kumar, S., and Finotello, D., 1994, *Phys. Rev. Lett.*, **73,** 2708.

[3] Crawford, G. P., Yang, D. K., Žumer, S., Finotello, D., and Doane, J. W., 1991, *Phys. Rev. Lett.*, **66,** 723; Crawford, G. P., Ondris-Crawford, R. J., Doane, J. W., and Žumer, S., 1996, *Phys. Rev. E*, **53,** 3647 and references therein; Ziherl, P., Vilfan, M., Vrbančič-Kopač, N., Žumer, S., Ondris-Crawford, R. J., and Crawford, G. P., 2000, *Phys. Rev. E*, **61,** 2792.

[4] Guyot-Sionnest, P., Hsiung, H., and Shen, Y. R., 1986, *Phys. Rev. Lett.*, **57,** 2963; Huang, J. Y., Superfine, R., and Shen, Y. R., 1990, *Phys. Rev. A*, **42,** 3660; Zhuang, X., Marrucci, L., and Shen, Y. R., 1994, *Phys. Rev. Lett.*, **73,** 1513; Qian, T., Zhuang, X., and Shen, Y. R., 1999, *Phys. Rev. E*, **59,** 1873.

[5] Nicholson, J. P., 1988, *J. Phys. Fr.*, **49,** 2111; Chen, W., Martinez-Miranda, L. J., Hsiung, H., and Shen, Y. R., 1989, *Phys. Rev. Lett.*, **62,** 1860; Hsiung, H., Rasing, Th., and Shen, Y. R., 1986, *Phys. Rev. Lett.*, **57,** 3065.

[6] Foster, J. S., and Frommer, J. E., 1988, *Nature*, **333,** 542; Walba, D. M., Stevens, F., Parks, D. C., Clark, N. A., and Wand, M. D., 1995, *Science*, **267,** 1144.

[7] Horn, R. G., Israelachvili, J. N., and Perez, E., 1981, *J. Physique*, **42,** 39.

[8] Clark, N. A., 1985, *Phys. Rev. Lett.*, **55,** 292; Ouchi, Y., Feller, M. B., Moses, T., and Shen, Y. R., 1992, *Phys. Rev. Lett.*, **68,** 3040.

[9] Muševič, I., Slak, G., and Blinc, R., 1996, *Rev. sci. Instr.*, **67,** 2554.

[10] Israelachvili, J., 1992, *Intermolecular and Surface Forces* (Academic Press).

[11] De Gennes, P. G., 1990, *Langmuir*, **6,** 1448.

[12] Borštnik, A., Stark, H., and Žumer, S., 1999, *Phys. Rev. E*, **60,** pp. 4210.

[13] Johnson, K. L., 1985, *Contact Mechanics* (Cambridge University Press).

[14] Sheng, P., 1976, *Phys. Rev. Lett.*, **37,** 1059; Miyano, K., 1979, *Phys. Rev. Lett.*, **43,** 51; Tarzcon, J. C., and Miyano, K., 1981, *Phys. Rev. Lett.*, **46,** 119; Yokoyama, H., Kobayashi, S., and Kamei, H., 1982, *Appl. Phys. Lett.*, **41,** 438; Poniewierski, A., and Sluckin, T. J., 1987, *Liq. Cryst.*, **2,** 281; Sluckin, T. J., and Poniewierski, A., 1990, *Mol. Cryst. liq. Cryst.*, **179,** 349.

[15] Moreau, L., Richetti, P., and Barois, P., 1994, *Phys. Rev. Lett.*, **73,** 3556; Richetti, P., Moreau, L., Barois, P., and Kekicheff, P., 1996, *Phys. Rev. E*, **54,** 1749.

[16] Davidov, D., Safinya, C. R., Kaplan, M., Dana, S. S., Schaetzing, R., Birgenau, R. J., and Litster, J. D., 1979, *Phys. Rev. B*, **19,** 1657; Gierlotka, S., Lambooy, P., and de Jeu, W. H., 1990, *Europhys. Lett.*, **12,** 341.